第16卷第11期
2026年11月

中国无机分析化学
Chinese Journal of Inorganic Analytical Chemistry

Vol. 16, No. 11
2048～2056

**doi: 10. 20236/j. CJIAC. 2026. 11. 008**

朱斌, 李亚举, 李晶蓉, 等. 基于激光诱导击穿光谱(LIBS)结合互信息-偏最小二乘回归的铀矿石中铀的定量分析[J]. 中国无机分析化学, 2026, 16(11): 2048-2056.

Zhu Bin, Li Yaju, Li Jingrong, et al. Quantitative Analysis of Uranium in Uranium Ore by Laser-induced Breakdown Spectroscopy (LIBS) Combined with Mutual Information-Partial Least Squares Regression[J]. Chinese Journal of Inorganic Analytical Chemistry, 2026, 16(11): 2048-2056.

# 基于激光诱导击穿光谱(LIBS)结合互信息-偏最小二乘回归的铀矿石中铀的定量分析

朱 斌[1] 李亚举[2*] 李晶蓉[3] 杭玉桦[1] 隋明达[1]
梅金娜[1] 钱东斌[4] 曾 强[4] 刘小亮[3*]

(1. 苏州热工研究院有限公司, 江苏 苏州 215004;
2. 先进能源科学与技术广东省实验室, 广东 惠州 516000;
3. 东华理工大学 核科学与工程学院, 南昌 330013;
4. 中国科学院 近代物理研究所, 兰州 730000)

**摘 要** 铀矿石中铀含量的快速准确测定对铀矿勘探现场快速决策与品位鉴定具有重要意义。针对铀矿石基体复杂、谱线干扰严重导致传统单变量分析准确度低的问题, 本文提出了一种基于互信息(MI)特征筛选结合偏最小二乘回归(PLSR)的激光诱导击穿光谱(LIBS)高精度定量分析方法。以10个铀质量分数跨度为200～45 300 μg/g的铀矿石样品为研究对象, 采用标准正态变量变换(SNV)结合Savitzky-Golay (SG)平滑对原始光谱进行预处理, 以消除样品间散射差异并滤除高频随机噪声。基于预处理后的光谱, 分别构建了单变量、全谱PLSR及MI-PLSR三种定量模型, 并系统对比了其分析性能。结果表明, 单变量模型在低含量端(S3样品, 1 390 μg/g)预测严重偏离真实值, 相对误差(RE)高达897. 99%; 而在高含量端(S7样品, 15 100 μg/g)的RE为5. 69%。预测性能呈现明显的含量依赖性, 整体可靠性不足。当利用全部54 102个波长变量构建全谱PLSR模型时, 其校准曲线的决定系数$R^2$为0. 999 84, 预测均方根误差($RMSE_P$)为1 834 μg/g; 经MI筛选后, 采用38 000个特征变量构建MI-PLSR模型, 其$R^2$提升至0. 999 93, $RMSE_P$降至1 601 μg/g。在低含量端, 两种多变量模型的预测准确度基本相当, RE分别为5. 69%和6. 03%; 而在高含量端, MI-PLSR有效抑制了过拟合风险, RE由采用全谱时的10. 95%降至7. 76%。本研究证实, LIBS结合多变量校准策略有效提高了复杂铀矿石中铀元素的分析性能, 可为铀矿资源的现场快速定量分析提供有益参考。

**收稿日期:** 2026-08-12 **修回日期:** 2026-08-20 **录用日期:** 2026-08-21 **在线出版日期:** 2026-08-25

**Received:** 2026-08-12 **Revised:** 2026-08-20 **Accepted:** 2026-08-21 **Online published:** 2026-08-25

**基金项目:** 国家自然科学基金资助项目(12365021, 12005037); 东江实验室科技计划项目(DJL2025C006)

**Fund:** Supported by the National Natural Science Foundation of China (12365021, 12005037); Dongjiang Laboratory S & T Program (DJL2025C006)

**作者简介:** 朱斌, 男, 高级工程师, 主要从事基于激光的材料表征技术研究与装备开发工作。E-mail: zhu. bin@cgnpc. com. cn

**Author:** Zhu Bin, male, senior engineer, mainly engaged in research on laserbased material characterization techniques and equipment development. E-mail: zhu. bin@cgnpc. com. cn

***通信作者:** 李亚举, 男, 助理研究员, 主要从事激光光谱检测技术、激光与物质相互作用等方面的研究。E-mail: liyaju@gdlhz. ac. cn
刘小亮, 男, 副教授, 主要从事激光光谱检测技术等方面的研究。E-mail: 201960177@ecut. edu. cn

***Corresponding author:** Li Yaju, male, assistant professor, mainly engaged in research on laserinduced breakdown spectroscopy (LIBS) and lasermatter interaction. E-mail: liyaju@gdlhz. ac. cn

Liu Xiaoliang, male, associate professor, mainly engaged in research on laserbased spectroscopic detection techniques. E-mail: 201960177@ecut. edu. cn

©Chinese Journal of Inorganic Analytical Chemistry Editorial Department 2026. This is an open access article under the CC-BY-NC-ND 4.0 License.

**关键词**　激光诱导击穿光谱；铀矿石；偏最小二乘回归；互信息；定量分析

**要点**

1）LIBS结合MI-PLSR实现铀矿石中铀元素高准确度定量分析。

2）多变量校准策略有效补偿基体效应，显著改善低含量端预测准确度。

3）MI特征筛选降低过拟合，全含量范围预测性能优于全谱PLSR。

**中图分类号**：O657.38　TD983　　**文献标志码**：A　　**文章编号**：2095-1035(2026)11-2048-09

铀矿石是核工业的基础原料，铀(U)含量的准确测定对于铀矿资源评估、选冶工艺优化及辐射安全防护具有重要意义。目前，铀矿石中铀含量的常规分析方法包括电感耦合等离子体质谱法(ICP-MS)[1]、电感耦合等离子体发射光谱法(ICP-OES)[2]及X射线荧光光谱法(XRF)[3]等，这些方法虽精度较高，但样品前处理繁琐、分析周期长，难以满足铀矿勘探现场对快速检测的需求。

激光诱导击穿光谱(Laser-induced Breakdown Spectroscopy，LIBS)利用高能脉冲激光烧蚀样品产生等离子体，通过采集其辐射光谱实现元素分析[4-6]。与传统方法相比，LIBS具有无需复杂预处理、分析速度快、可原位在线检测等优势，已广泛应用于矿石分析[7]、冶金工程[8]及环境监测[9-10]等领域。然而，当分析对象为天然铀矿石时，LIBS的分析准确性会受到基体效应的严重制约。一方面，矿石中Fe、V、Mn、Al等共存基体元素的发射谱线丰富，极易对铀的特征谱线造成干扰[11-12]。另一方面，不同品位矿石在硬度、密度、含水率等理化性质上差异显著，导致基体效应的非线性程度远超一般矿石体系。此外，铀元素激发效率较低，在低含量区间特征谱线信噪比偏低，有效信号易被背景噪声掩盖[13-14]。在此条件下，传统依赖单一特征谱线强度的单变量定标法，因无法利用全谱信息进行基体补偿，其定量结果常严重偏离真实值，进而难以满足实际分析需求。

为克服单变量方法的固有局限，多变量校准策略被逐步引入LIBS定量分析[15-19]。其中，偏最小二乘回归(Partial Least Squares Regression，PLSR)通过对光谱矩阵和含量矩阵同时进行正交分解，可有效处理波长变量间的高度共线性问题，已成为LIBS多变量建模的常用工具[20-22]。已有研究表明，PLSR能够利用多波长信息抑制矿石基体干扰，在铜矿石、铁矿石及稀土矿石等体系中均取得优于单变量校准的分析效果[23-24]。然而，LIBS光谱通常包含数万个波长变量，而实际研究中可获取的标准样品数量往往十分有限。在此“高维小样本”数据结构下，直接将全部波长变量输入PLSR模型，极易引入大量与目标元素无关的背景信息和仪器噪声，造成模型过拟合，严重制约泛化能力[25]。因此，如何在保留有效光谱信息的前提下合理压缩变量空间、剔除冗余干扰，是全谱PLSR策略在矿石LIBS分析中亟待解决的关键问题。

特征降维与变量筛选是解决上述矛盾的有效技术路径[26-28]。其中，基于互信息(Mutual Information，MI)的滤波式特征选择方法以信息熵为理论基础，能够量化任意两个随机变量间的相互依赖程度，对线性与非线性关系均具有良好的感知能力，且不依赖任何先验数据分布假设[29-30]。相较于相关系数等线性度量指标，MI在LIBS这类信号强度与元素含量之间可能呈现非线性响应关系的体系中更具适用优势。近年来，MI已在LIBS应用场景中展现出良好的特征筛选效果[31-32]。将MI与PLSR相结合，理论上可在保留与目标含量高度相关的关键变量的同时压缩模型输入维度，从而在全谱PLSR框架内实现模型复杂度与预测精度的平衡。

本研究以10个铀质量分数跨度为200～45 300 μg/g的铀矿石样品为研究对象，在大气环境中采用LIBS对铀含量进行定量分析。采用标准正态变量变换(SNV)结合Savitzky-Golay(SG)平滑进行光谱预处理，在此基础上系统对比单变量校准、全谱PLSR及MI-PLSR三种建模策略的分析性能，旨在评估LIBS在铀矿石定量分析中的预测性能与实际效用，以期为复杂基体矿石中铀元素的快速分析提供方法学参考。

## 1　实验原理与方法

### 1.1　样品制备

实验以江西某铀矿区围岩为基体，其本底铀含量经ICP-MS测定为80 μg/g。围岩经粉碎、研磨、过筛后得到均匀粉末，再采用加标混合法将硝酸铀酰[$UO_2(NO_3)_2$]标准溶液按设计含量逐级滴加至上述粉末中，在涡旋振荡器中充分混匀，使铀盐均匀分散。随后将混合物置于电热恒温干燥箱中在80 ℃下烘干至恒重，以彻底去除水分。烘干后的样品经玛

瑙研钵研磨至均匀粉末，确保铀元素在基体中的分布均匀性。将处理后的粉末置于不锈钢模具中，在8 MPa压力下保压3 min，压制成直径20 mm、厚度约2.5 mm的圆片(单片质量约2.0 g)。所有制备操作均在洁净实验台中进行，每种配比样品使用独立称量纸与器具，以避免交叉污染。制备所得样品铀含量范围为200～45 300 μg/g，并按铀含量由低至高依次编号为S1－S10，各样品编号及对应铀含量见表1。制备好的样品在测量前保存于干燥箱中，以确保稳定性。

**表1 样品编号及铀元素含量**

**Table 1 Sample numbers and the corresponding uranium concentrations** /(μg·g$^{-1}$)

| Reference | Sample No. | | | | | | | | | |
|---|---|---|---|---|---|---|---|---|---|---|
| | S1 | S2 | S3 | S4 | S5 | S6 | S7 | S8 | S9 | S10 |
| U | 200 | 1 030 | 1 390 | 2 260 | 4 530 | 7 580 | 15 100 | 27 000 | 39 500 | 45 300 |

### 1.2 光谱采集

本研究采用的LIBS实验系统主要由激光器、中阶梯光谱仪、ICCD探测器、三维自动化样品台及数据采集处理系统组成。其中，激光器(DPS-1064-BS-D-100 mJ，希爱)输出波长为1 064 nm，单脉冲能量设为50 mJ，重复频率为10 Hz。激光束经焦距150 mm的石英透镜垂直聚焦于样品表面，为避免空气击穿，焦点置于样品表面下方约1 mm处，焦斑直径约为250 μm。光谱仪(ARYELLE Butterfly，LTB，德国)配备ICCD探测器(Andor，DH334T)，探测范围为190～430 nm，分辨本领$\lambda/\Delta\lambda$为50 000，探测延迟和曝光宽度分别设为2和20 μs。测量时，每个样品选取60个测量点(点间距0.5 mm)，每个点采集50个连续激光脉冲的累积光谱。10个样品共采集600张原始光谱，其中S3和S7作为预测集，其余8个样品作为训练集用于建模。所有光谱采集均在室温(25±1) ℃、相对湿度(45%±5%)和常压(约101.3 kPa)的实验室环境中进行，以最大限度降低环境因素对实验结果的干扰。

### 1.3 模型构建

本研究的数据分析与建模流程如图1所示。首先，采用SNV结合SG平滑算法对原始光谱进行预处理，以消除样品间散射差异并滤除高频随机噪声。随后，基于预处理光谱分别开展两类定量分析策略的研究：一是单变量校准模型，即提取特定分析线的特征谱线构建定标曲线；二是多变量校准模型，包括通过8折交叉验证确定最优潜变量个数的全谱PLSR模型，以及结合MI特征筛选与8折交叉验证构建的MI-PLSR模型。最后，采用决定系数($R^2$)、均方根误差(RMSE)和相对误差(RE)等指标对各模型的分析结果进行综合评价[33]，全面对比3种模型对矿石基体效应的补偿效果，并验证MI筛选在提升模型预测性能方面的作用。

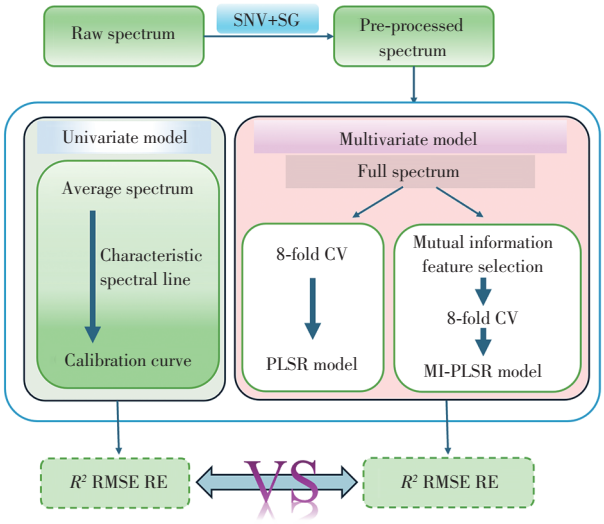



**图1 铀矿石铀含量定量分析建模流程图**

**Figure 1 Workflow of quantitative analysis modeling for uranium concentration in uranium ores.**

## 2 结果与讨论

### 2.1 铀矿石的LIBS光谱

实验获取了10个铀矿石样品各60次重复测量的LIBS光谱，每个光谱包含54 102个波长变量。其中，S5样品经过SNV＋SG预处理后的平均LIBS光谱如图2所示。根据美国国家标准与技术研究院(NIST)的光谱数据库对采集到的LIBS光谱进行谱线识别。从图2中可以看出，光谱中强度较高的谱线主要来自基体中的Fe、V、Mn、Al等元素，而能明确识别的铀谱线较少，仅U Ⅱ 280.25、311.16、385.95 nm 3条。其中，U Ⅱ 311.16 nm与Fe Ⅰ 311.16 nm存在严重谱线重叠，U Ⅱ 385.95 nm附近则分布着V、Ti、Cu、Th等多条干扰线，两者都难以直接用于定标曲线的构建；唯有U Ⅱ 280.25 nm谱线受邻近干扰较少，谱峰形貌清晰、相对独立。因此选取U Ⅱ 280.25 nm作为后续单变量建模的分析线。

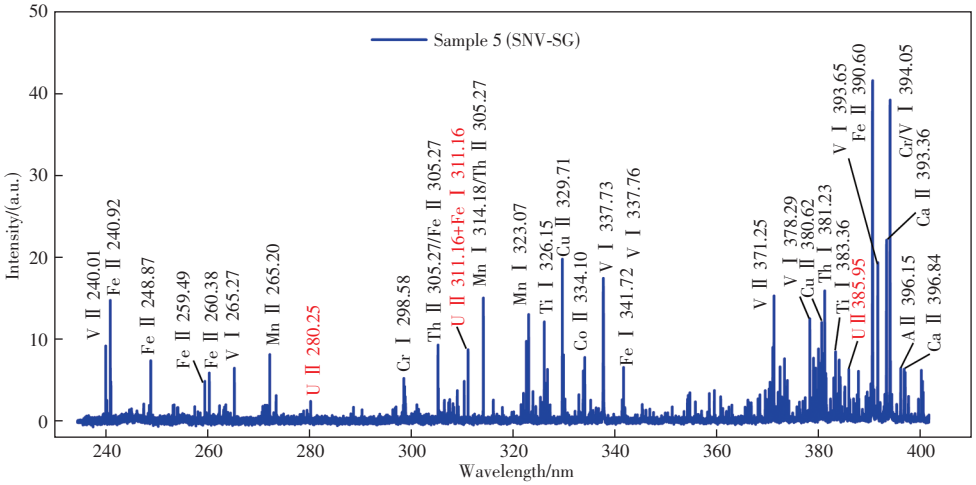



**图2　5号铀矿石样品预处理后的LIBS光谱图**

**Figure 2　LIBS spectrum of S5 uranium ore sample after preprocessing.**

## 2.2　单变量分析

由图3a可知，原始光谱(RAW)受基体效应影响，特征峰强度与铀含量未呈现出明显的单调响应，如S6样品的峰强度反而高于S10样品。经SNV+SG预处理后，样品间的散射差异得以校正，高频噪声被有效滤除，各样品分析线的强度随铀含量增加整体呈现单调递增趋势。基于预处理后的分析线峰面积构建全含量范围的线性校准曲线，如图3b所示。模型的定标方程为 $Y=0.00057896X+9.17701$，决定系数 $R^2$ 为0.858 06，表明该模型的线性拟合效果不够理想。为评估其实际预测能力，将该模型应用于S3(1 390 μg/g)和S7(15 100 μg/g)两个独立预测样本。结果显示，模型对S7的预测相对误差为5.69%，预测值与参考值较为接近；但对S3的预测值严重偏离真实含量，预测得出 −11 092.19 μg/g的负值，相对误差高达897.99%。这种偏差主要源于两方面原因：一方面，低含量样本的谱峰强度接近基线噪声水平，信噪比不足，导致峰面积提取的准确性较差；另一方面，校准曲线方程主要由高含量样本决定，低含量区域的样本点较少，模型在该区间缺乏有效约束，外推时产生不可靠的预测结果。上述结果表明，在矿石基体复杂、含量范围跨度大的情况下，单变量校准策略难以保证全含量范围内的预测准确性和可靠性。

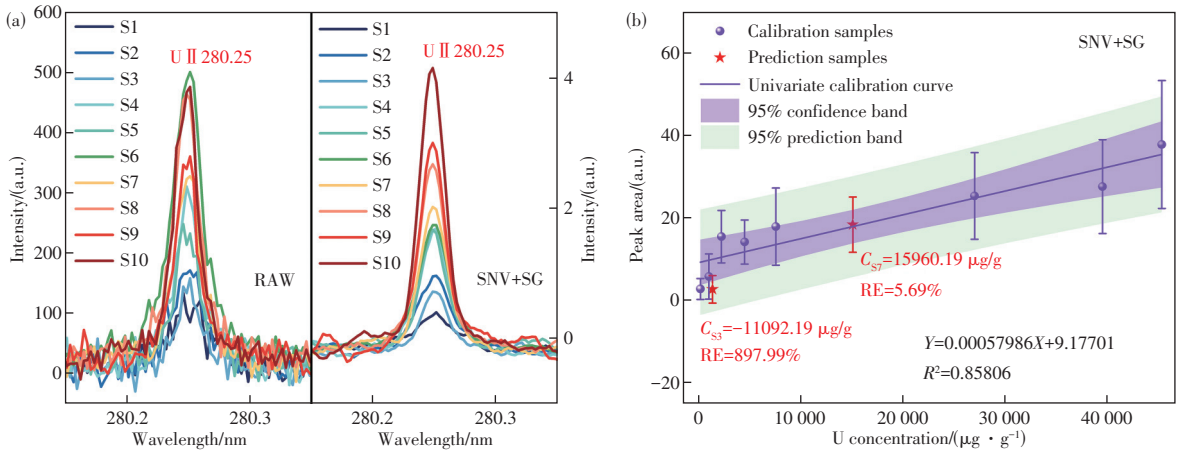



**图3　(a)原始与SNV+SG预处理特征光谱；(b)SNV+SG预处理光谱单变量定标曲线及预测集误差**

**Figure 3　(a) Raw characteristic spectra and SNV+SG preprocessed spectra; (b) Univariate calibration curve for SNV+SG preprocessed spectra and the prediction set errors.**

### 2.3 PLSR模型结果分析

为了克服单变量校准的局限性，本研究通过PLSR构建了全谱多变量定量模型。模型优化采用8折交叉验证法确定最优潜变量($LV_s$)个数，以交叉验证均方根误差($RMSE_{CV}$)最低为评价标准。全谱PLSR模型的$RMSE_{CV}$随潜变量个数的变化如图4a所示。当潜变量个数为10时，$RMSE_{CV}$达到最小值，此时全谱PLSR模型预测结果如图4b所示。该模型的训练集均方根误差$RMSE_C$为1 116.5446 μg/g，预测集均方根误差$RMSE_P$为1 834.421 8 μg/g，决定系数$R^2$达0.999 84。相比于单变量模型，全谱PLSR显著改善了全含量范围内的预测效果，其中S3的预测含量为1 469.05 μg/g，RE为5.69%，有效纠正了单变量模型中的严重负值偏差；S7的预测含量为16 753.72 μg/g，RE为10.95%。因此，PLSR多变量模型能够通过全谱范围的信息互补，有效补偿复杂矿石基体效应带来的非线性响应，展现出优异的整体定量分析性能[34-35]。然而，全谱数据中仍包含大量与铀元素无关的背景信息或高频噪声，直接以全谱作为输入可能导致模型对训练集噪声信息产生过拟合，这在一定程度上削弱了其泛化能力，$RMSE_P$仍偏高。因此，为了进一步精简模型架构、降低过拟合风险，有必要在多元建模前引入特征优化策略。

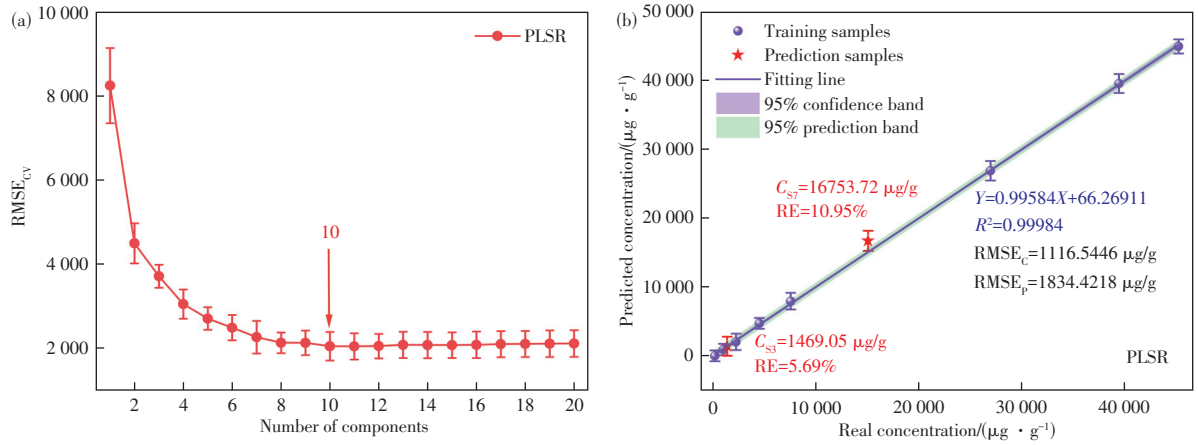



**图4 (a)$RMSE_{CV}$随潜变量个数的变化曲线；(b)铀元素预测含量与真实含量的线性拟合图**

**Figure 4 (a) Variation curve of $RMSE_{CV}$ with the number of latent variables; (b) Linear fitting plot between predicted and actual concentrations of uranium.**

### 2.4 MI-PLSR模型结果分析

为了降低全光谱PLSR模型中的变量冗余，引入MI算法对光谱特征变量进行筛选。基于训练集光谱计算各波长变量与铀含量MI值并降序排列，通过遍历多组候选特征数量，结合8折交叉验证与单标准误准则确定全局最优特征子集。MI-PLSR模型的$RMSE_{CV}$随筛选特征数的变化如图5a所示。经优化确定最优特征个数为38 000，$LV_s$为9。图5b展示了基于最优参数条件下构建的MI-PLSR定量模型的校准曲线，其$RMSE_C$为1 245.80 μg/g，$RMSE_P$降低至1 600.98 μg/g，决定系数$R^2$提升至0.999 93。此时，S3的预测含量为1 473.83 μg/g，RE为6.03%；S7的预测含量为16 271.08 μg/g，RE为7.76%。MI算法通过评估各波长变量与铀含量间的统计依赖程度，筛选并保留信息量丰富的特征变量，有效弱化了背景变量在多元线性组合中的噪声放大效应，从而在更精简的模型架构下实现了全含量范围内预测性能的提升。为直观对比3种模型对独立测试样的预测性能，将各模型对低含量预测样S3和高含量预测样S7的分析结果汇总于表2。由表2可知，单变量模型在低含量端完全失效，相对误差高达897.99%；两种多变量模型在低含量端预测性能相当，而MI-PLSR在高含量端的$RMSE_P$为1 846.51 μg/g，RE为7.76%，均优于全谱PLSR对应的2 199 μg/g和10.95%，表明MI特征筛选在保持低含量预测能力的同时，有效提升了高含量端的预测准确度。

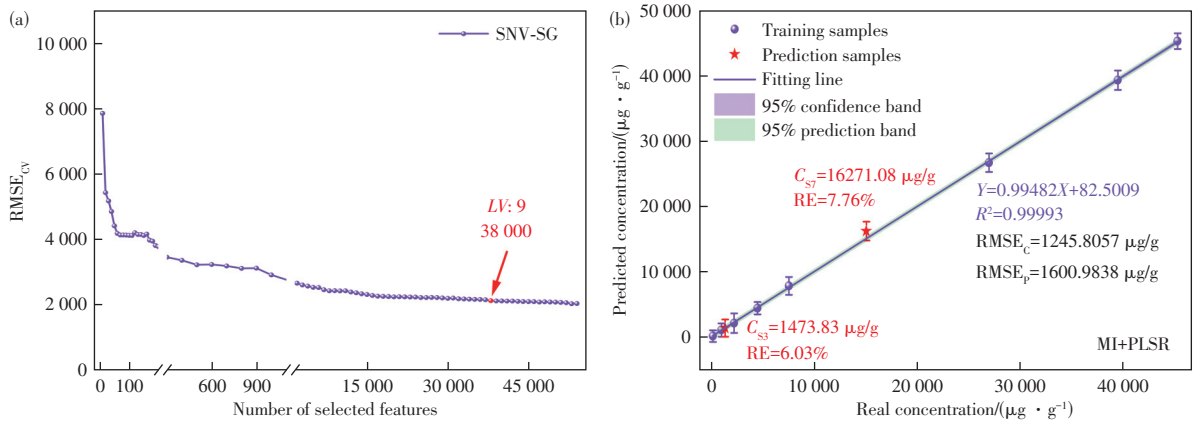



**图5　(a) $RMSE_{CV}$ 随筛选特征数变化曲线；(b) 铀元素预测含量与真实含量的线性拟合图**

**Figure 5　(a) Variation curve of $RMSE_{CV}$ with the number of selected features; (b) Linear fitting plot between predicted and actual concentrations of uranium element.**

**表2　不同定量模型分析结果对比**

**Table 2　Comparison of quantitative analysis results for different models**

| Test sets | Methods | Predicted values/(μg · g$^{-1}$) | $R^2$ | $RMSE_P$/(μg · g$^{-1}$) | RE/% |
|---|---|---|---|---|---|
| 1 390 | Univariate | −11 092. 19 | 0. 858 06 | 13 730. 78 | 897. 99 |
| | PLSR | 1 469. 05 | 0. 999 84 | 1 376. 44 | 5. 69 |
| | MI-PLSR | 1 473. 83 | 0. 999 93 | 1 310. 22 | 6. 03 |
| 15 100 | Univariate | 15 960. 19 | 0. 858 06 | 11 483. 26 | 5. 69 |
| | PLSR | 16 753. 72 | 0. 999 84 | 2 199 | 10. 95 |
| | MI-PLSR | 16 271. 08 | 0. 999 93 | 1 846. 51 | 7. 76 |

## 3　结论

本文采用LIBS技术结合单变量校准、全谱PLSR及MI-PLSR 3种策略，对铀矿石中铀元素进行定量分析。研究表明，在基体复杂的铀矿石体系中，单变量模型受谱线重叠和基体效应制约，难以兼顾宽含量范围的分析需求；全谱PLSR通过多波长信息互补有效补偿了基体干扰，但高维输入引入的冗余信息会导致模型在高含量端预测误差较大；而MI-PLSR通过MI筛选剔除低相关性变量，在保持低含量良好预测能力的同时显著提升了高含量端的预测准确度，在全含量范围内具有更好的预测准确度和泛化能力。本研究证实，LIBS结合多变量校准策略可有效提高复杂铀矿石中铀元素的定量分析性能，为铀矿资源的现场快速评价提供了方法学参考。后续工作将进一步扩充样品数量与基体类型，并引入非线性建模策略，以提升模型的泛化能力与普适性。

### 参考文献

[1]　曾江萍，王家松，朱悦，等. 敞开酸溶-电感耦合等离子体质谱法测定铀矿石中15种稀土元素[J]. 岩矿测试，2022，41(5)：789-797.
Zeng Jiangping，Wang Jiasong，Zhu Yue，et al. Determination of 15 rare earth elements in uranium ore by open acid dissolution-inductively coupled plasma-mass spectrometry[J]. Rock and Mineral Analysis，2022，41(5)：789-797.

[2]　解原，黄浩，成景特，等. 超声雾化-ICP-OES法测定铀矿尾渣中低含量的铀和钍[J]. 化学工程师，2020，34(5)：32-34.
Xie Yuan，Huang Hao，Cheng Jingte，et al. Determination of low-content uranium and thorium in uranium ore tailings by ICP-OES with ultrasonic nebulization[J]. Chemical Engineer，2020，34(5)：32-34.

[3]　袁建，刘香英，夏晨光，等. 熔融制样-X射线荧光光谱法测定产铀岩石中钨、钼、铌、钽、铁、磷、钒的标准方法[J]. 核化学与放射化学，2017，39(5)：362-367.
Yuan Jian，Liu Xiangying，Xia Chenguang，et al. Standard method for determination of W，Mo，Nb，Ta，Fe，P，V in uranium-productive rock by X-ray fluorescence spectrometry[J]. Journal of Nuclear and Radiochemistry，2017，39(5)：362-367.

[4]　Hussain Shah S K，Iqbal J，Ahmad P，et al. Laser induced breakdown spectroscopy methods and applications：

a comprehensive review[J]. Radiation Physics and Chemistry, 2020, 170: 108666. DOI: 10.1016/j.radphyschem.2019.108666.

[5] Guo Lianbo, Zhang Deng, Sun Lanxiang, et al. Development in the application of laser-induced breakdown spectroscopy in recent years: a review[J]. Frontiers of Physics, 2021, 16(2): 22500. DOI: 10.1007/s11467-020-1007-z.

[6] Thomas J, Chandra Joshi H. Review on laser-induced breakdown spectroscopy: methodology and technical developments[J]. Applied Spectroscopy Reviews, 2024, 59(1): 124-155.

[7] Liu Jingzhong, Zhang Rongling, Li Qiao, et al. PLS regression-assisted LIBS for simultaneous quantitative analysis of five REEs and TREOs in rare earth ores[J]. Journal of Analytical Atomic Spectrometry, 2026, 41(6): 2117-2126.

[8] 牛广辉, 张业建, 林庆宇. 激光诱导击穿光谱(LIBS)技术在低碳钢铁冶金行业的应用[J]. 中国无机分析化学, 2024, 14(2): 168-175.
Niu Guanghui, Zhang Yejian, Lin Qingyu. Application of laser-induced breakdown spectroscopy in low-carbon steel metallurgy industry[J]. Chinese Journal of Inorganic Analytical Chemistry, 2024, 14(2): 168-175.

[9] Zhang Ying, Zhang Tianlong, Li Hua. Application of laser-induced breakdown spectroscopy (LIBS) in environmental monitoring[J]. Spectrochimica Acta Part B: Atomic Spectroscopy, 2021, 181: 106218. DOI: 10.1016/j.sab.2021.106218.

[10] 李业秋, 孙成林, 李倩, 等. 大气颗粒物中重金属的双脉冲激光诱导击穿光谱研究[J]. 红外与激光工程, 2019, 48(10): 1005006. DOI: 10.3788/IRLA201948.1005006.
Li Yeqiu, Sun Chenglin, Li Qian, et al. Analysis of the heavy metals in atmospheric particulate matter using dual-pulsed laser-induced breakdown spectroscopy[J]. Infrared and Laser Engineering, 2019, 48(10): 1005006. DOI: 10.3788/IRLA201948.1005006.

[11] Zhang Mengjia, Li Hao, Deng Luan, et al. High-accuracy and efficient classification of uranium slag by origin and category via LIBS integrated with hybrid machine learning[J]. Sensors, 2026, 26(8): 2522. DOI: 10.3390/s26082522.

[12] 舒开强, 许应铜, 高智星, 等. 激光诱导击穿光谱对U元素的定量分析[J]. 中国无机分析化学, 2024, 14(2): 139-144.
Shu Kaiqiang, Xu Yingtong, Gao Zhixing, et al. Quantitative analysis of uranium in uranium ore by laser-induced breakdown spectroscopy combined with machine learning[J]. Chinese Journal of Inorganic Analytical Chemistry, 2024, 14(2): 139-144.

[13] Li Qingzhou, Zhang Wen, Tang Zhiyang, et al. Determination of uranium in ores using laser-induced breakdown spectroscopy combined with laser-induced fluorescence[J]. Journal of Analytical Atomic Spectrometry, 2020, 35(3): 626-631.

[14] Ji Jianxun, Song Weiran, Hou Zongyu, et al. Raw signal improvement using beam shaping plasma modulation for uranium detection in ore using laser-induced breakdown spectroscopy[J]. Analytica Chimica Acta, 2022, 1235: 340551. DOI: 10.1016/j.aca.2022.340551.

[15] Hao Zhongqi, Liu Ke, Lian Qianlin, et al. Machine learning in laser-induced breakdown spectroscopy: a review[J]. Frontiers of Physics, 2024, 19(6): 62501. DOI: 10.1007/s11467-024-1427-2.

[16] 闫红宇, 赵宇, 陈媛媛, 等. 远程LIBS结合GA-arPLS的爆炸物识别研究[J]. 光谱学与光谱分析, 2024, 44(11): 3199-3205.
Yan Hongyu, Zhao Yu, Chen Yuanyuan, et al. Explosive residue identification study by remote LIBS combined with GA-arPLS[J]. Spectroscopy and Spectral Analysis, 2024, 44(11): 3199-3205.

[17] Huang Qian, Yu Haoyang, Jiang Zhaohui, et al. Multi-component quantitative analysis of LIBS using adaptively optimized multi-branch CNN[J]. Optics & Laser Technology, 2024, 179: 111282. DOI: 10.1016/j.optlastec.2024.111282.

[18] Lyu Yihan, Song Wenrui, Hou Zhaoyang, et al. Incorporating empirical knowledge into data-driven variable selection for quantitative analysis of coal ash content by laser-induced breakdown spectroscopy[J]. Plasma Science and Technology, 2024, 26(7): 075509. DOI: 10.1088/2058-6272/ad370c.

[19] Huang Y, Bais A, Mohajan S, et al. Adaptive learning with logistic regression for soil classification with LIBS[C]//2024 IEEE International Conference on Plasma Science (ICOPS). Beijing, 2024: 1.

[20] Khalaji M, Mohajan S, Karimi S, et al. Multivariate calibration of nanoparticle-enhanced LIBS (NELIBS) for gold nanoparticle quantification[J]. Sensors and Actuators A: Physical, 2026, 409: 118089. DOI: 10.1016/j.sna.2026.118089.

[21] Yoon S, Choi J, Moon S J, et al. Determination and quantification of heavy metals in sediments through laser-induced breakdown spectroscopy and partial least squares regression[J]. Applied Sciences, 2021, 11(15): 7154. DOI: 10.3390/app11157154.

[22] Liu Xiangqian, Yan Chunhua, An Duanyang, et al. Rapid quantitative analysis of rare earth elements Lu and Y in

rare earth ores by laser induced breakdown spectroscopy combined with iPLS-VIP and partial least squares[J]. RSC Advances, 2023, 13(22): 15347-15355.

[23] Brinkmann P, Köllner N, Merk S, et al. Comparison of handheld and echelle spectrometer to assess copper in ores by means of laser-induced breakdown spectroscopy (LIBS)[J]. Minerals, 2023, 13(1): 113. DOI: 10.3390/min13010113.

[24] Jia Jinwei, Liu Zefeng, Pan Chengyu, et al. Detection of Al, Mg, Ca, and Zn in copper slag by LIBS combined with calibration curve and PLSR methods[J]. Plasma Science and Technology, 2024, 26(2): 025507. DOI: 10.1088/2058-6272/ad1045.

[25] Ma Qing, Liu Ziyuan, Sun Tong, et al. Small-sample stacking model for qualitative analysis of aluminum alloys based on femtosecond laser-induced breakdown spectroscopy[J]. Optics Express, 2023, 31(17): 27633. DOI: 10.1364/oe.497880.

[26] Mehmood T, Liland K H, Snipen L, et al. A review of variable selection methods in Partial Least Squares Regression[J]. Chemometrics and Intelligent Laboratory Systems, 2012, 118: 62-69.

[27] Chun H, Keleş S. Sparse partial least squares regression for simultaneous dimension reduction and variable selection[J]. Journal of the Royal Statistical Society Series B: Statistical Methodology, 2010, 72(1): 3-25.

[28] Yan Chunhua, Liang Jing, Zhao Mingjing, et al. A novel hybrid feature selection strategy in quantitative analysis of laser-induced breakdown spectroscopy[J]. Analytica Chimica Acta, 2019, 1080: 35-42.

[29] Vergara J R, Estévez P A. A review of feature selection methods based on mutual information[J]. Neural Computing and Applications, 2014, 24(1): 175-186.

[30] Cheng Jiehong, Sun Jun, Yao Kunshan, et al. A variable selection method based on mutual information and variance inflation factor[J]. Spectrochimica Acta Part A: Molecular and Biomolecular Spectroscopy, 2022, 268: 120652. DOI: 10.1016/j.saa.2021.120652.

[31] Ruan Fangqi, Hou Lin, Zhang Tianlong, et al. A novel hybrid filter/wrapper method for feature selection in archaeological ceramics classification by laser-induced breakdown spectroscopy[J]. The Analyst, 2021, 146(3): 1023-1031.

[32] He Ting, Liang Jing, Tang Hongsheng, et al. Quantitative analysis of coal quality by mutual information-particle swarm optimization (MI-PSO) hybrid variable selection method coupled with spectral fusion strategy of laser-induced breakdown spectroscopy (LIBS) and Fourier transform infrared spectroscopy (FTIR)[J]. Spectrochimica Acta Part B: Atomic Spectroscopy, 2021, 178: 106112. DOI: 10.1016/j.sab.2021.106112.

[33] Zhang Youjian, Zhang Xiong, Ma Yiwen, et al. Quantitative analysis of coal quality by laser-induced breakdown spectroscopy assisted with different chemometric methods[J]. Analytical Methods, 2020, 12(27): 3530-3536.

[34] Liu Xiaoliang, Ren Shichao, Zhang Ming, et al. Comparison of nanosecond and femtosecond laser-induced breakdown spectroscopy for determination of U and Th in tantalum-niobium ores[J]. Journal of Analytical Atomic Spectrometry, 2025, 40(2): 437-446.

[35] Akhmetzhanov T F, Labutin T A, Korshunov D M, et al. Determination of Ce and La in REE-rich ores using handheld LIBS and PLS regression[J]. Journal of Analytical Atomic Spectrometry, 2023, 38(10): 2134–2143.

# Quantitative Analysis of Uranium in Uranium Ore by Laser-induced Breakdown Spectroscopy (LIBS) Combined with Mutual Information-Partial Least Squares Regression

Zhu Bin[1], Li Yaju[2*], Li Jingrong[3], Hang Yuhua[1], Sui Mingda[1], Mei Jinna[1], Qian Dongbin[4], Zeng Qiang[4], Liu Xiaoliang[3*]

(*1. Suzhou Nuclear Power Research Institute Co., Ltd., Suzhou, Jiangsu 215004, China;*
*2. Advanced Energy Science and Technology Guangdong Laboratory, Huizhou, Guangdong 516000, China;*
*3. School of Nuclear Science and Engineering, East China University of Technology, Nanchang, Jiangxi 330013, China;*
*4. Institute of Modern Physics, Chinese Academy of Sciences, Lanzhou, Gansu 730000, China*)

**Abstract** The rapid and accurate quantification of uranium in ores is critically important for on-site decision-making and grade identification during uranium exploration. However, the accuracy of conventional univariate

calibration methods is often compromised by the complex matrix composition and severe spectral line interferences of uranium ores. To address this issue, a high-precision quantitative approach based on laser-induced breakdown spectroscopy (LIBS) combined with mutual information (MI) feature selection and partial least squares regression (PLSR) is proposed. Ten uranium ore samples with uranium mass fractions ranging from 200 to 45 300 μg/g were investigated. The raw LIBS spectra were preprocessed using standard normal variate (SNV) transformation followed by Savitzky-Golay (SG) smoothing to eliminate inter-sample scattering variations and suppress high-frequency random noise. On the basis of the preprocessed spectra, the quantitative performances of univariate calibration, full-spectrum PLSR, and MI-PLSR were systematically compared. A severe deviation was observed for the low-concentration sample (S3, 1 390 μg/g) with the univariate model, for which the relative error (RE) was as high as 897.99%, whereas for the high-concentration sample (S7, 15 100 μg/g) the RE was 5.69%. This marked concentration-dependent behavior indicates inadequate overall reliability of the univariate approach. In contrast, from the full-spectrum PLSR model constructed using all 54 102 wavelength variables, a calibration coefficient of determination ($R^2$) of 0.999 84 and a root-mean-square error of prediction ($RMSE_P$) of 1 834 μg/g were obtained. After MI-based feature selection, an improved $R^2$ of 0.999 93 and an $RMSE_P$ of 1 601 μg/g were achieved with the MI-PLSR model built with 38 000 selected variables. For the low-concentration sample, essentially comparable prediction accuracies were delivered by both multivariate models, with RE values of 5.69% and 6.03%, respectively. For the high-concentration sample, the overfitting risk observed in the full-spectrum PLSR was effectively mitigated by MI-PLSR, and the RE was reduced from 10.95% to 7.76%. It is confirmed that LIBS combined with multivariate calibration strategies has effectively improved the quantitative analysis performance of uranium in complex ores, and a useful reference for rapid on-site quantitative analysis of uranium resources can thereby be provided.

**Keywords** laser-induced breakdown spectroscopy; uranium ore; partial least squares regression; mutual information; quantitative analysis

**HIGHLIGHTS**

1) LIBS coupled with MI-PLSR was applied to achieve quantitative analysis of uranium in uranium ores.
2) Multivariate calibration effectively compensates matrix effects and markedly enhances prediction accuracy for low-concentration samples.
3) MI-based feature selection alleviates overfitting, and exhibits better prediction performance across the whole concentration range than full-spectrum PLSR.